

See discussions, stats, and author profiles for this publication at: <https://www.researchgate.net/publication/264157732>

Structural Analysis of Single Wall Carbon Nanotubes Exposed to Oxidation and Reduction Conditions in the Course of Gamma Irradiation

ARTICLE in THE JOURNAL OF PHYSICAL CHEMISTRY C · JULY 2014

Impact Factor: 4.77 · DOI: 10.1021/jp502685n

READS

53

9 AUTHORS, INCLUDING:



S. Jovanović

Vinča Institute of Nuclear Sciences

31 PUBLICATIONS 384 CITATIONS

[SEE PROFILE](#)



Miroslav D Dramicanin

Vinča Institute of Nuclear Sciences

281 PUBLICATIONS 1,955 CITATIONS

[SEE PROFILE](#)



Ivanka Holclajtner-Antunović

University of Belgrade

99 PUBLICATIONS 428 CITATIONS

[SEE PROFILE](#)



Zois Syrgiannis

ITM-CNR, Padua, Italy

33 PUBLICATIONS 212 CITATIONS

[SEE PROFILE](#)

Structural Analysis of Single Wall Carbon Nanotubes Exposed to Oxidation and Reduction Conditions in the Course of Gamma Irradiation

Svetlana P. Jovanović,^{*,†} Zoran M. Marković,[†] Duška N. Kleut,[†] Miroslav D. Dramićanin,[†] Ivanka D. Holclajtner-Antunović,[‡] Momir S. Milosavljević,[†] Valeria La Parola,[§] Zois Syrgiannis,^{||} and Biljana M. Todorović Marković[†]

[†]Vinča Institute of Nuclear Sciences, University of Belgrade, P.O. Box 522, 11001 Belgrade, Serbia

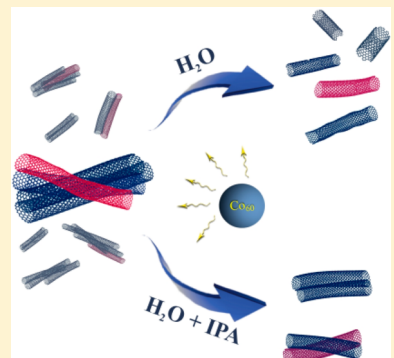
[‡]Faculty of Physical Chemistry, University of Belgrade, P.O. Box 47, 11158 Belgrade, Serbia

[§]Istituto per lo Studio dei Materiali Nanostrutturati (ISMN-CNR), I-90146 Palermo, Italy

^{||}Department of Chemical and Pharmaceutical Sciences, INSTM, Center of Excellence for Nanostructured Materials (CENMAT), University of Trieste, 34127 Trieste, Italy

Supporting Information

ABSTRACT: Single wall carbon nanotubes (SWCNTs) were exposed to gamma irradiation in oxidative (H_2O , NH_4OH) and reductive (H_2O and NH_4OH both mixed with isopropyl alcohol) media. The structure has been investigated with microscopic (atomic force and transmission electron microscopy), spectroscopic (Raman, X-ray photoelectron, and FTIR spectroscopy) techniques, and by thermogravimetric analysis. Reductive media offer the possibility for green chemistry reduction of SWCNTs: after gamma irradiation, SWCNTs lose C–O bonds. Furthermore, irradiation in these media increases the fraction of sp^2 hybridized carbon atoms in structure of SWCNTs and prevents their amorphization. The presence of isopropyl alcohol in reductive media contributed to the preservation of structure's unity. On the other hand, the most effective procedure is the one that occurs in oxidative media and yields in debundled, cut, and annihilated carbon nanotubes. The smaller diameter and the metallic ones are the most affected.



1. INTRODUCTION

Because of their unique properties, single walled carbon nanotubes (SWCNTs) have drawn scientist's great attention in diverse research fields such as physics, chemistry, biology, medicine, etc.^{1–7} High aspect ratio and hollow structure of SWCNTs make them a promising agent for drug delivery,⁸ sensing applications,^{9,10} nanosorbents for removal of contaminants in drinking water,¹¹ agents in a photothermal therapy, etc.^{12–14} Major obstacles in the processing of SWCNTs are the intrinsic solubility in any type of solvent and the fact that the production techniques yield a mixture in terms of length and diameter. Their chemical functionalization is recognized as the key to overcome this obstacle.³ Apart from the conventional methods regarding the chemical transformation of the carbon nanotubes, nonstandard techniques such as gamma irradiation have recently appeared in the literature.^{15,16} Gamma irradiation seems to have found wide application in the functionalization of multi walled carbon nanotubes (MWCNTs).^{17,18} A linear relationship between the amount of gamma irradiation and the introduction of functional moieties and defects on MWCNTs has been reported. Taking advantage of these findings, several groups have been able to functionalize the sidewalls of MWCNT with polymer chains, by simply applying gamma

rays to monomer–MWCNT mixtures.^{19,20} We have also established that gamma irradiation is a very useful pretreatment in the process of noncovalent functionalization of SWCNTs with DNA.²¹ Hulman et al. have shown that gamma irradiation creates defects and destroys the coherence motion of C atoms on the nanotube circumference.²² Moreover, our previous research has shown that an irradiation dose of 100 kGy can yield to the decrease of the SWCNT length of about 50%.²³ Except for the functionalization and the cutting effects, certain media for gamma irradiation can cause the decrease of interwall distance in MWCNT structure and the improvement of their graphitic order or, on the contrary, the increase of the interwall distance of MWCNTs and the structure disorder.^{24,25} Li et al. have shown that when the irradiation dose exceeds 200 kGy, the defect dynamics is changed and the nanotubes are annealed.²⁶

In this work, SWCNTs were gamma irradiated in two different types of media: with and without the presence of isopropyl alcohol (IPA). IPA was added as a quencher of $\cdot OH$

Received: March 18, 2014

Revised: May 29, 2014

radicals, which are produced in water and ammonia solution during irradiation.^{27–29} Herein are presented the occurred structural changes and the relevance of various experimental parameters that were being used. Specifically the larger diameter SWCNTs are affected more under irradiation in oxidative media, while no real change took place in reductive ones. The approach can be used for reducing the amount of different diameters in each batch of SWCNTs.

2. EXPERIMENTAL SECTION

Purified SWCNTs (diameter 0.75–2 nm, length 4 μm, 95% purity) were purchased from Bucky Corp. (Houston, TX). A first group of samples was obtained by irradiation of nanotubes in oxidative media: SWCNTs (30 mg) were sonicated with 30 mL of MilliQ water (γ -OxW-SWCNTs) or with 30 mL of 30% ammonia solution (γ -OxA-SWCNTs). The second group of samples was obtained by irradiation in reductive media: 30 mg of SWCNTs was sonicated with 2 mL of IPA and 30 mL of MilliQ water (γ -RedW-SWCNTs) or with 2 mL of IPA and 30 mL of 30% ammonia solution (γ -RedA-SWCNTs). A number of prepared samples were irradiated by gamma ray flux from ^{60}Co nuclide with the photon energy of 1.3 MeV (Centre of Irradiation, Vinča Institute of Nuclear Sciences) at the dose rate of 10 kGy h⁻¹. The samples were exposed to the source of gamma irradiation absorbing the doses of 25, 50, and 100 kGy. From this point, irradiation dose will be indicated as a subscript in the sample name ($_{25}\gamma$ -OxW-SWCNTs, $_{50}\gamma$ -OxW-SWCNTs, $_{100}\gamma$ -OxW-SWCNTs, and the same rule for other samples). After irradiation treatment, nanotube powders were air-dried at 80 °C.

Nanotube powders were dissolved in *o*-dichlorobenzene (*o*-DCB) at a concentration of 50 mg/L. A dispersion of pristine and gamma irradiated SWCNTs was sonicated (ultrasonic bath with power 750 W) for 3 h. As substrate, we used Ag deposited on glass (Ag/glass). Nanotube dispersions were spin-coated on Ag/glass substrate and then dried at 200 °C. These thin films were used for Raman measurements.

Raman spectra of gamma irradiated SWCNT films were obtained by a DXR Raman microscope (Thermo Scientific) with the use of two lasers: 532 nm excitation line with a maximum constant power of 2 mW and spot size of 0.7 μm on the sample while the spectral resolution was 0.5 cm⁻¹; 780 nm excitation line, maximum constant power of 2 mW and spot size 2.1 μm and the spectral resolution was 1 cm⁻¹. All Raman spectra were recorded at five different locations on each sample, and at each spot the recording was repeated three times. Raman spectroscopy measurements were conducted at room temperature. Acquisition time was 200 s (20 × 10 s) for all samples.

The X-ray photoelectron spectroscopy (XPS) analyses were performed with a VGMicrotech ESCA 3000 Multilab, equipped with a dual Mg/Al anode. The samples were excited by the unmonochromatized Al K α source (1486.6 eV) run at 14 kV and 15 mA. The analyzer was operated in the constant analyzer energy (CAE) mode. For the individual peak energy regions, a pass energy of 20 eV set across the hemispheres was used. Survey spectra were measured at 50 eV pass energy. The sample powders were analyzed as powder, mounted on a double-sided adhesive tape. The pressure in the analysis chamber was in the range of 10⁻⁸ Torr during data collection. The constant charging of the samples was removed by referencing all of the energies to the C 1s set at 284.4 eV, on the main C 1s peak of SWCNTs. The invariance of the peak

shapes and widths at the beginning and at the end of the analyses ensured absence of differential charging. Analyses of the peaks were performed with the software provided by VG, based on nonlinear least-squares fitting program using a weighted sum of Lorentzian and Gaussian component curves after background subtraction according to Shirley and Sherwood. Atomic concentrations were calculated from peak intensity using the sensitivity factors provided with the software. The binding energy values are quoted with a precision of ±0.15 eV and the atomic percentage with a precision of ±10%.

For Fourier transform infrared spectroscopy (FTIR), SWCNT powders mixed with KBr powder and pellets were formed. Measurements were conducted at room temperature in a spectral range from 400 to 4000 cm⁻¹ in transmittance mode, on a Nicolet 380 FTIR, Thermo Electron Corp. spectrometer.

The thermal stability of pristine and gamma irradiated SWCNTs was examined by thermogravimetric analysis (TGA) by using a Mettler Toledo TGA/DSC STAR System. The measurements were conducted at a heating rate of 10 °C/min in a dynamic nitrogen ($\varphi = 30$ mL/min) and air atmosphere ($\varphi = 30$ mL/min).

Dispersions of gamma irradiated carbon nanotubes in *o*-DCB were observed by transmission electron microscopy (TEM, JEOL JEM 2010F) with field-emission electron source and operated at 200 kV. Nanotube dispersions were drop-casted on grids. As a substrate, we used carbon-coated grids, purchased from SPI Supplies, USA.

Atomic force microscopy (AFM) measurements were performed by the use of Quesant microscope operating in tapping mode in air at room temperature. Nanotube dispersions in *o*-dichlorobenzene were deposited on mica substrate and imaged after drying. Standard spin-coating equipment at 4000 rpm was used for sample depositions. Silicon tips (purchased from Nano and More) with constant force of 40 N/m were used. The height of nanotubes was measured with Gwyddion software. For height histograms, 100 nanotube bundles were measured in each sample.

3. RESULTS AND DISCUSSION

3.1. Raman Analysis of Pristine and Gamma Irradiated SWCNTs.

Raman spectroscopy is a very important tool for

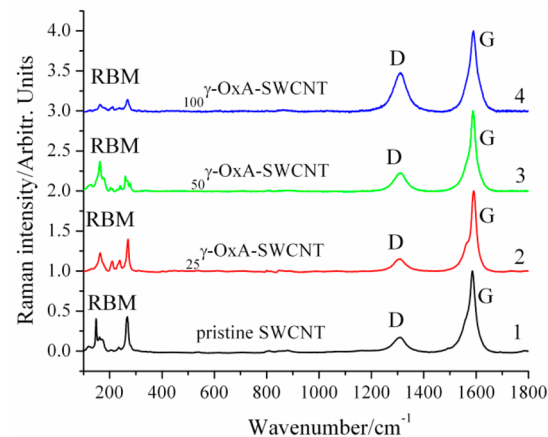


Figure 1. Raman spectra of pristine SWCNTs (1), $_{25}\gamma$ -OxA-SWCNTs (2), $_{50}\gamma$ -OxA-SWCNTs (3), and $_{100}\gamma$ -OxA-SWCNTs (4) samples at a laser wavelength of 780 nm. Spectra have been normalized and vertically displaced for clarity.

Table 1. D- and G-Bands' Positions (in cm^{-1}), and Normalized $I_{\text{D}}/I_{\text{G}}$ Ratios for Pristine and Gamma Irradiated SWCNTs, $\lambda = 780 \text{ nm}$

sample	position of D-band	position of G-band	$I_{\text{D}}/I_{\text{G}}$ ratio
pristine SWCNTs	1313	1587	1.00
25γ -OxW-SWCNTs	1312	1589	0.95
25γ -OxA-SWCNTs	1308	1591	0.74
25γ -RedW-SWCNTs	1306	1586	1.17
25γ -RedA-SWCNTs	1307	1585	1.25
50γ -OxW-SWCNTs	1308	1588	1.06
50γ -OxA-SWCNTs	1311	1588	1.04
50γ -RedW-SWCNTs	1305	1585	1.50
50γ -RedA-SWCNTs	1307	1586	1.49
100γ -OxW-SWCNTs	1306	1584	2.20
100γ -OxA-SWCNTs	1307	1587	2.95
100γ -RedW-SWCNTs	1308	1586	1.64
100γ -RedA-SWCNTs	1306	1586	1.40

investigating the changes in SWCNT structure.^{30,31} In Figure 1, Raman spectra of pristine and irradiated SWCNTs at doses of 25, 50, and 100 kGy in aqua ammonia are displayed. In all spectra, three groups of bands appear: radial breathing mode (RBM) is in the range of 100–300 cm^{-1} , and it corresponds to radial expansion–contraction of the nanotube; D-band is the result of disorder in nanotube sidewalls and is located at around

1350 cm^{-1} ; and graphitic or G-band stems from highly ordered nanotube structures at 1580 cm^{-1} (Figure 1). All Raman spectra have been normalized with respect to the intensity of the G-band.

To quantitatively measure the amount of defects in SWCNT, produced by gamma irradiation, the intensity ratios of D- and G-bands ($I_{\text{D}}/I_{\text{G}}$) are adequate. Table 1 shows the positions of D- and G-bands, as well as the normalized $I_{\text{D}}/I_{\text{G}}$ ratios for all SWCNT samples. For the laser excitation line of 532 nm, the values of the same parameter are listed in Table S1 (Supporting Information).

In Raman spectra of pristine SWCNTs, D-band has the maximum at 1313 cm^{-1} (Table 1). The D-band intensity is a result of a decrease in the structural order in the SWCNT. The position of D-band is downshifted for all gamma irradiated SWCNTs. Clear enhancement of the D-band intensity is observed with increasing defect density or with decreasing nanotube lengths.³² The frequency of D-band is inversely proportional to the nanotube diameter.³³ The D-band frequency linearly decreases with the increasing of gamma irradiation dose for nanotubes irradiated in oxidative media. Moreover, for SWCNTs irradiated in reductive media, D-band frequency downshifts nearly 7 cm^{-1} for all of the applied doses. Thus, the gamma irradiated SWCNTs in the reductive media are having the same effect no matter what the amount of the irradiation dose. The shift of the D-band frequency can be explained as the result of the change in nanotube diameters. For irradiated SWCNTs, diameters increase or remain constant

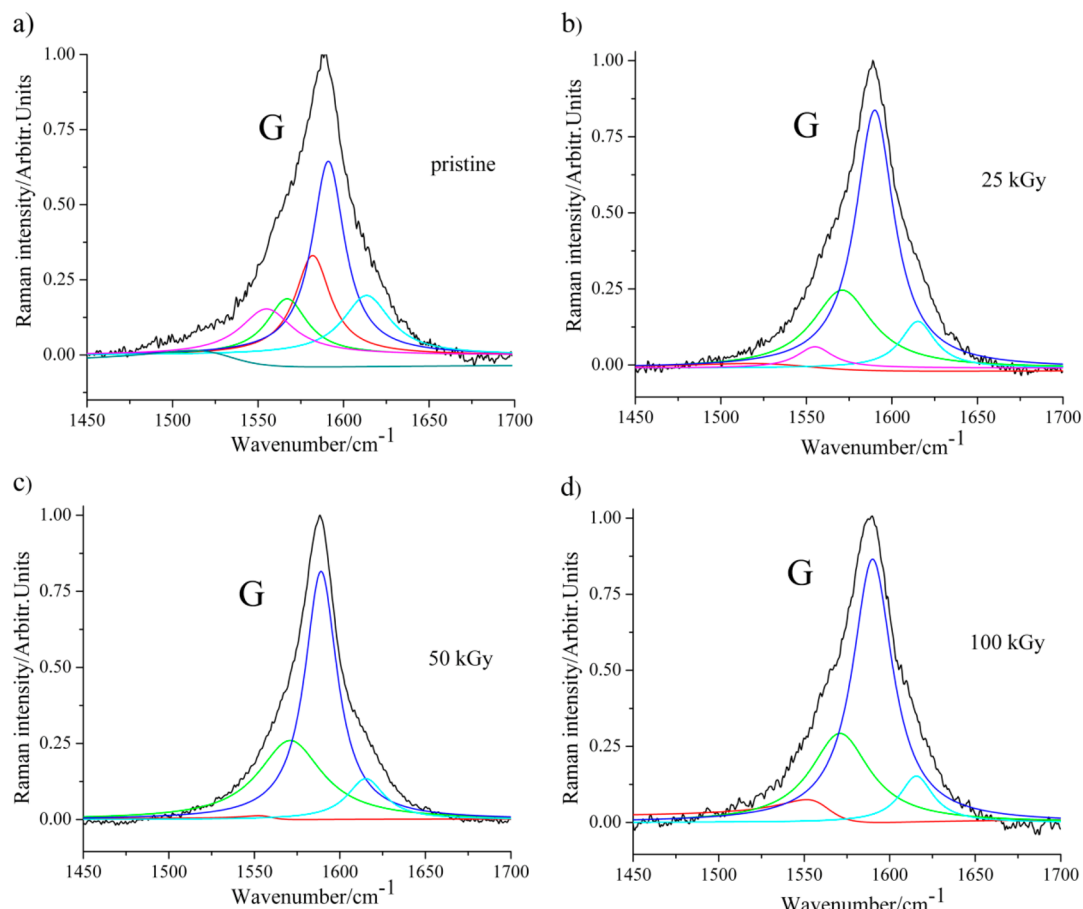


Figure 2. Deconvolutions of G-band of Raman spectra of pristine SWCNTs (a), 25γ -OxW-SWCNTs (b), 50γ -OxW-SWCNTs (c), and 100γ -OxW-SWCNTs (d), $\lambda = 780 \text{ nm}$.

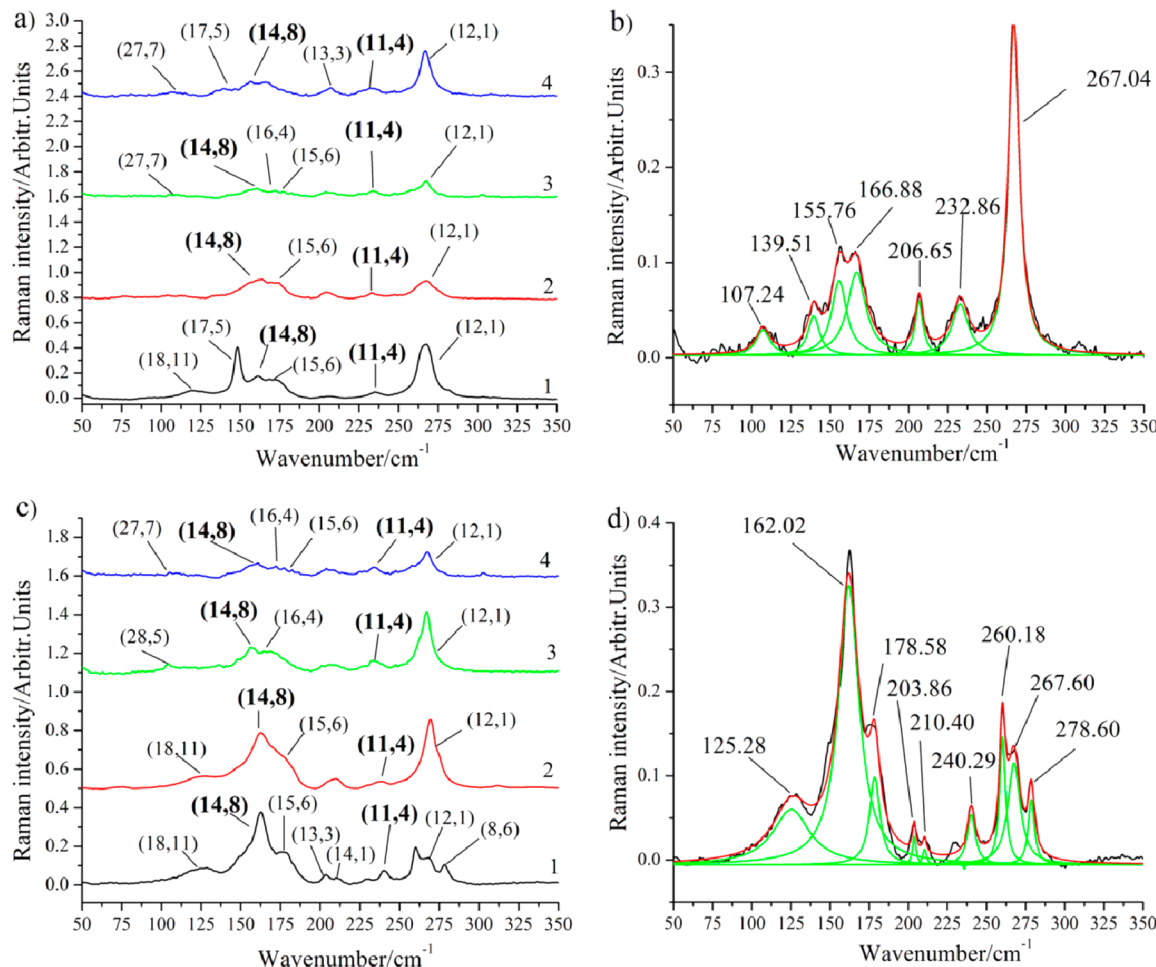


Figure 3. (a) RBM regions of Raman spectra of pristine SWCNTs (1), 25γ -RedW-SWCNTs (2), 50γ -RedW-SWCNTs (3), and 100γ -RedW-SWCNTs (4), the numbers indicate the (n,m) types; (b) RBM bands of 100γ -RedW-SWCNTs sample fitted with seven Lorentzian functions; (c) RBM regions of 50γ -OXA-SWCNTs (1), 50γ -OxW-SWCNTs (2), 50γ -RedA-SWCNTs (3), and 50γ -RedW-SWCNTs (4), the numbers indicate the (n,m) types; and (d) fitted RBM region for 50γ -OXA-SWCNTs with nine Lorentzian functions. Spectra (a) and (c) have been normalized and vertically displaced for clarity ($\lambda = 780$ nm).

depending on the dose of irradiation and also on the environment.

For nanotubes irradiated in oxidative media with a dose of 25 kGy, the I_D/I_G ratios were slightly lower than that of pristine nanotubes; this can be explained by a cleaning effect of the pristine material. During irradiation, media such as water and aqua ammonia are decomposed into reactive oxidative species. These species can react with the residual amorphous carbon and cause oxidation. Amorphous carbon has a large amount of reactive edges in structure, which are exposed directly to oxidizing agents upon irradiation. Therefore, amorphous carbon is being oxidized before carbon nanotubes. At 50 kGy, the I_D/I_G ratio is enhanced in comparison to the value of the I_D/I_G ratio of pristine SWCNTs. At this dose, the structural modification of SWCNT sidewalls has most likely occurred. Hydroxyl radical and hydrogen peroxide, formed in media during irradiation, can oxidize SWCNTs and cause attachment of carboxyl and hydroxyl groups on the sidewalls. After irradiation at 100 kGy, the samples presented a high increase of I_D/I_G ratio, which, for the case of 100γ -OXA-SWCNTs, is almost 3 times the value of pristine SWCNTs. The large increase in structural disorder of irradiated nanotubes is probably the result of extensive nanotube oxidation and partial amorphization of SWCNTs.

The I_D/I_G ratio of the nanotubes irradiated in the reductive media also increases with every applied dose of the irradiation (Table 1). In detail, at 25 kGy, the I_D/I_G ratio significantly increased as compared to the pristine one. The I_D/I_G ratio further increases at 50 kGy, while at the dose of 100 kGy it reaches the highest value. The highest value of I_D/I_G ratio was noticed for 100γ -RedW-SWCNTs, which is 1.6 times higher as compared to pristine SWCNTs. These results indicate that in reductive media certain covalent modifications of SWCNTs took place at all applied doses. Considering that dominant reactive species are hydrogen, electron, and isopropyl radical, they could react with sp^2 C of SWCNTs. Hydrogen atoms or radical species can cause the breaking of C–C bonds and formation of new covalently attached groups on SWCNTs. At 100 kGy, the I_D/I_G ratio is significantly smaller for SWCNTs irradiated in reductive media as compared to those irradiated in oxidative media.

The fitting of the G-band of Raman spectrum of pristine SWCNTs is usually presented as a convolution of several peaks, which stem from metallic as well as semiconducting ones.^{34,35} It can be deconvoluted using six components, four semiconducting, Lorentzian features at positions 1553, 1569, 1592, and 1607 cm^{-1} and two metallic at 1540 and 1582

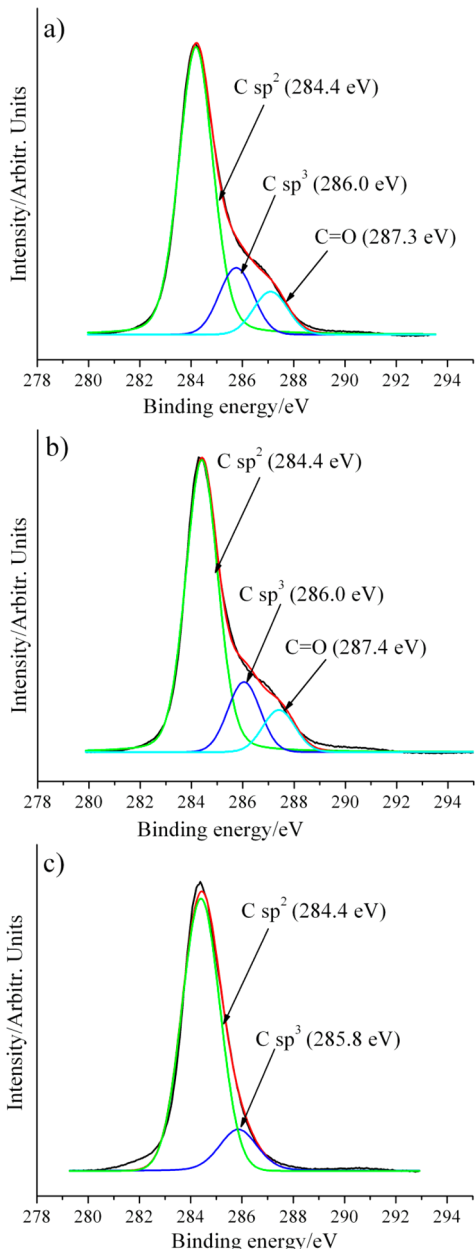


Figure 4. Deconvoluted C 1s XPS spectra of pristine SWCNTs (a), 100γ -OxA-SWCNTs (b), and 100γ -RedA-SWCNTs (c). The assignments of deconvoluted peaks are marked with arrows.

Table 2. O/C Atomic Ratios of Pristine and SWCNTs Irradiated in Oxidative and Reductive Media and Relative % of C 1s Components

sample	O/C ratio	C sp ² (%)	C sp ³ (%)	C=O (%)
pristine SWCNTs	0.03	74	16	10
100γ -RedA-SWCNTs	0.03	86	14	0
100γ -OxA-SWCNTs	0.02	74	16	10

cm⁻¹, of which one was Breit–Wigner–Fano (BWF) and the other Lorentzian.^{31,36}

All six characteristic features, in the G-band, were observed for pristine SWCNTs (Figure 2a), contrary to samples of SWCNTs irradiated in oxidative medium, Figures 2 (b–d).

In Figure 2 are depicted the G-band regions from the irradiated samples, collected at 780 nm wavelength excitation

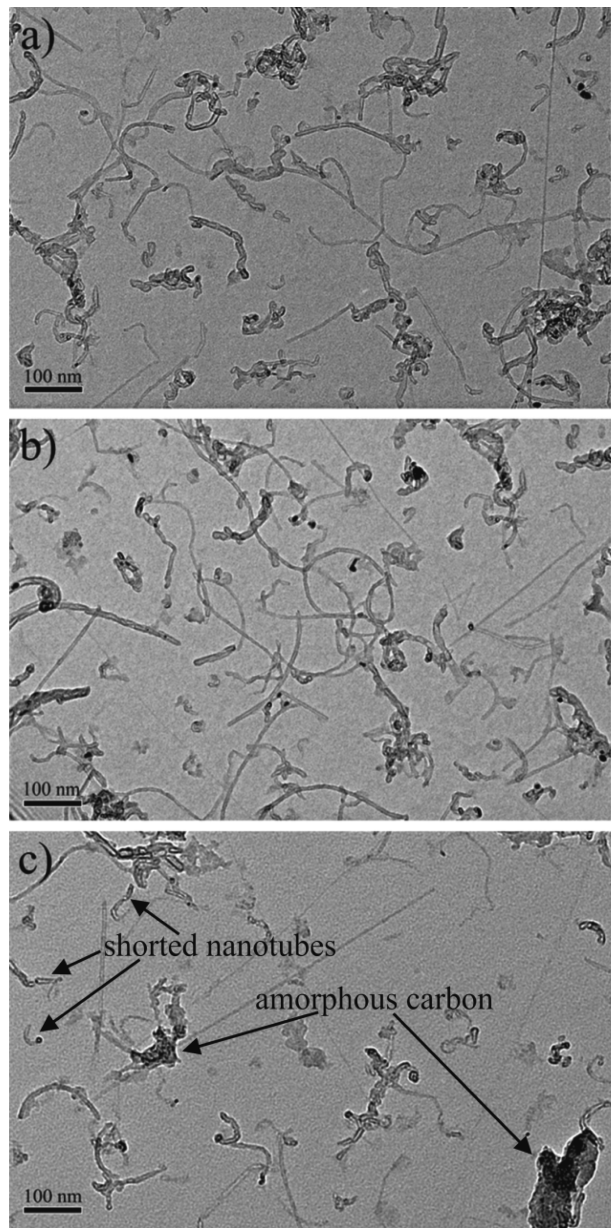


Figure 5. TEM micrographs of pristine SWCNTs (a), 100γ -RedW-SWCNTs (b), and 100γ -OxW-SWCNTs (c). Shortened SWCNTs and amorphous carbon are indicated with arrows.

laser, in oxidative media. These spectra (b–d) present a lack of the Lorentzian feature located at 1582 cm⁻¹, which corresponds to metallic SWCNTs. Also, the G-band feature at 1555 cm⁻¹ that corresponds to small diameter semiconducting SWCNTs is sustained only for the 25 kGy irradiation. By increasing the dose of the gamma irradiation, also this feature is quenched. Going one step further, we can assume that in oxidative media the metallic SWCNTs disappeared for all of the used doses and also that the higher doses yield to the quenching of the small diameter semiconducting SWCNTs. In the reductive media, G-band was fitted with five Lorentzians and one BWF, and they are presented in Table S2 (Supporting Information). Positions of G-band components are very similar to the corresponding values of pristine SWCNTs. However, for nanotubes irradiated in aqueous ammonia solution, all G-band features exist at all irradiation doses (Table S2, Supporting Information).

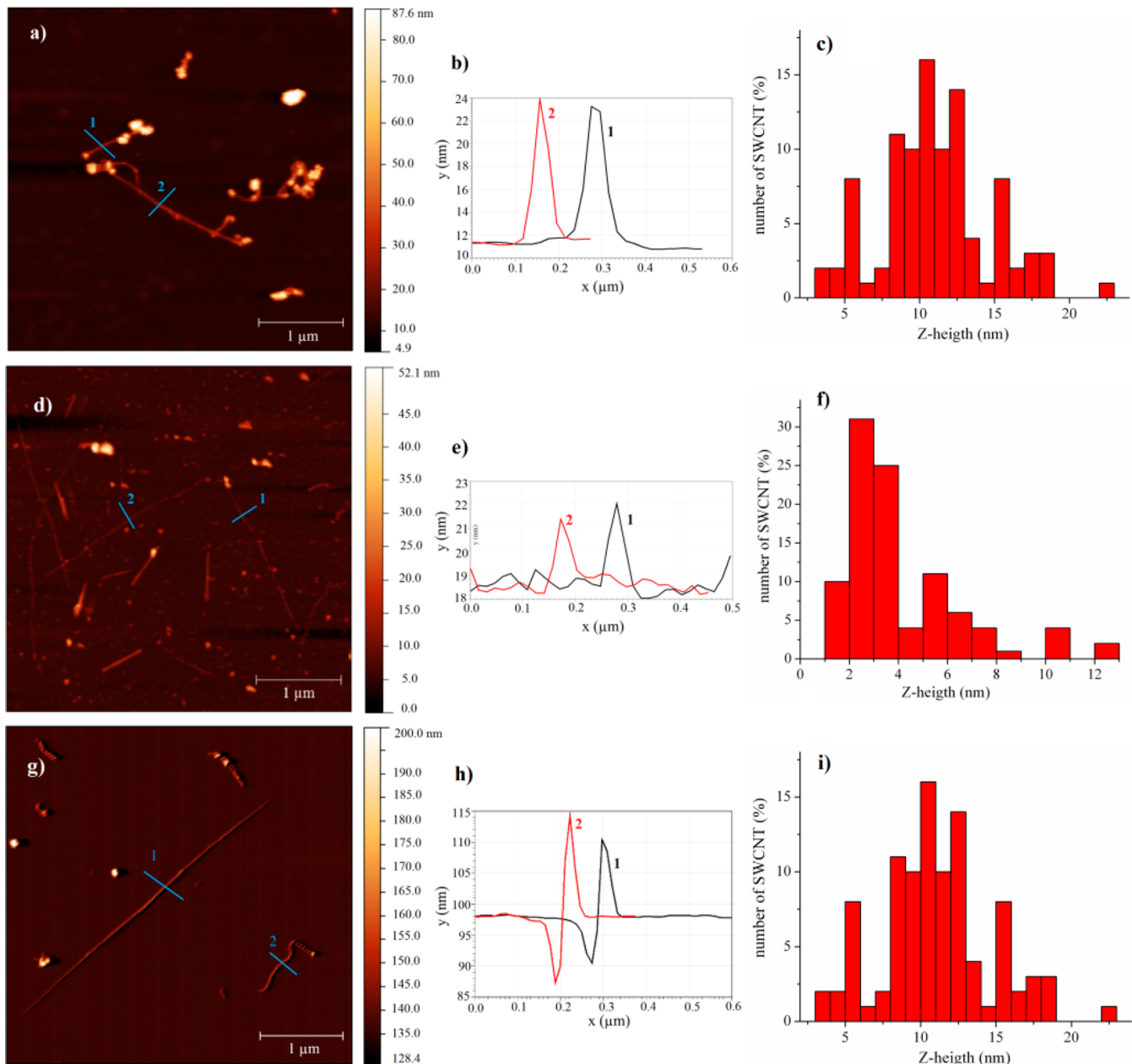


Figure 6. Top view AFM images with corresponding height profiles and height histograms for pristine (a–c), 50γ -Oxa-SWCNTs (d–f), and 50γ -RedA-SWCNTs (g–i), respectively.

The irradiation in water leads to the absence of certain Lorentzian features: at a dose of 25 kGy semiconducting feature at 1566.6 cm^{-1} and metallic at 1589.5 cm^{-1} ; at 50 kGy Lorentzian feature at 1613.3 cm^{-1} ; and at 100 kGy the component at 1553.8 cm^{-1} , both for semiconducting SWCNTs. This can be explained by the formation of active oxidation species such as hydroxyl radicals, hydroperoxyl radicals, and hydrogen peroxide, which can attack the scaffold of the SWCNTs.^{37,38} On the contrary, the use of IPA can prevent the destruction of nanotubes, due to the capacity of IPA to quench hydroxyl radicals in reductive media and to generate hydrogen, electrons, and other reduction species. During gamma irradiation, in the mixture of water with IPA, hydroxyl radicals react with IPA and form isopropyl radicals,²⁹ which are being reduced in nature. Hence, dominant species are reducing agents (hydrogen, electrons and isopropyl radicals). Therefore,

reductive media and the use of radical quenchers such as IPA can preserve sp^2 structure of SWCNTs during gamma irradiation.

The results of fitting analysis of the G-band region for Raman spectra collected at 532 nm excitation laser wavelength are listed in Table S3 (Supporting Information).

The final support to the previous results is coming from the elaboration of the RBM regions of pristine and gamma irradiated SWCNTs (Figure 3).

The analysis of RBM's peak position provides us with information about the diameters of the tubes. The following equation is commonly used for the diameter calculation of the SWCNTs: $\omega\text{ (cm}^{-1}\text{)} = 223.75/d\text{ (nm)} + 14\text{ cm}^{-1}$ ³⁹ The results of the fitting procedure from the RBM regions (positions, fwhm of bands, and diameters of identified SWCNTs) are depicted in Supporting Information Tables S4 and S5. The

(n,m) types of SWCNTs were determined with the use of the Kataura plot.⁴⁰

In oxidative media, SWCNTs with diameters less than and equal to 2.01 nm were detected (Table S4, Supporting Information). As is indicated in Figure 3c, the irradiation of the samples indicates a preference to smaller SWCNTs and also to the metallic nanotubes. The biggest diameter SWCNTs remained less affected (RBM region 250–275 cm⁻¹). These results are in correspondence with the aforementioned results.³⁹ On the other hand, as Figure 3a shows, the procedure in reductive media gives minor alterations in the RBM region. Moreover, it was noticed that RBM positions of certain features of the SWCNT in reductive media downshifted in opposition to their upshift in oxidative media. The aforementioned results can be concluded in the following points: (a) in oxidative media, we have selective destruction or functionalization of metallic tubes and also smaller diameter tubes with the further increase of the irradiation dose, (b) in reductive media, the nanotubes remain less affected, and (c) the use of IPA in aqueous solution concludes with the same results as in the case of the reductive media. What is needed to know after this analysis is the type of functional moieties on the carbon nanotube's scaffold.

3.2. Structural Analysis of Pristine and Gamma Irradiated SWCNTs. XPS is a very useful method for the investigation of the surface elemental composition of carbon nanotubes.^{41–43} It is used to investigate the chemical composition for both pristine and gamma irradiated SWCNTs. The curve fitting analyses of the C 1s region were carried out for the XPS spectra to quantify each functional group residing in pristine and gamma irradiated samples. Deconvolution of XPS spectra over the C 1s region from pristine and irradiated SWCNTs at a dose of 100 kGy in both the oxidative and the reductive is shown in Figure 4a–c, respectively.

In the XPS C 1s spectrum of pristine SWCNTs are identified three peaks. The main peak at 284.4 eV corresponds to the sp²-hybridized graphite-like carbon atoms (C=C) and is typical of graphitic carbon. The asymmetric tail at higher binding energy is due to the intrinsic defects on the SWCNT structures. The long tail of the main component was fitted with two peaks at ca. 286 and ca. 287.5 eV. The former component is generally assigned to C sp³, while the latter is assigned to oxygen contained species.^{41,43} The oxygen detected in pristine SWCNTs stems from oxidation during the process of acid purification.

The atomic ratios for pristine material and irradiated nanotubes in both oxidative and reductive media are summarized in Table 2.

The quantitative analysis indicates that after irradiation in both oxidative and reductive conditions, O/C ratios are very similar to that of pristine SWCNTs. Irradiation in reductive media caused the disappearance of the C=O component. On the contrary, the sample irradiated in oxidative condition showed a C 1s signal almost identical to the pristine SWCNT signal.

Deconvolution of the O 1s region gives additional information about the nature of oxygen-containing groups in structure of pristine and gamma irradiated SWCNTs. The curve fitting analyses of the O 1s region for all samples are shown in Figure S1 (Supporting Information). The spectrum of pristine SWCNTs is satisfactorily fitted with three components sited at 530.0, 532.3, and 534.4 eV. The two high energy components are attributed to C=O (ca. 532 eV) and C–O (ca. 534

eV),^{44,45} while the low energy component 530.0 is typical of metals oxides,^{46,47} and could be attributed to the impurities commonly present in the SWCNTs. Identical components were detected in samples irradiated in oxidative media, whereas in sample ¹⁰⁰γ-RedA-SWCNTs the component attributed to C–O disappeared (Supporting Information Figure S1.c). These groups were reduced with hydrogen atoms or electrons formed during irradiation in this medium.²⁹ XPS analysis of O 1s region confirmed that only the ¹⁰⁰γ-RedA-SWCNTs sample does not contain C–O bonds.

The structural changes of SWCNTs have also been studied by FTIR spectroscopy. FTIR spectra of pristine SWCNTs, ¹⁰⁰γ-RedA-SWCNTs, and ¹⁰⁰γ-OxA-SWCNTs are presented in Figure S2 (Supporting Information). The bands at 2830 and 2900 cm⁻¹ correspond to vibrations of C–H bonds in carbon nanotubes. Both pristine SWCNTs and ¹⁰⁰γ-OxA-SWCNTs show bands at 1080 and 1550 cm⁻¹, which are assigned to vibrations of C–OH from alkoxy and C–O from carboxyl functional groups, respectively (curves 1 and 3). These bands are not detected in the FTIR spectrum of ¹⁰⁰γ-RedA-SWCNTs (curve 2). All spectra show a band at 1720 cm⁻¹, which stems from vibration of C=O bonds in carboxyl functional groups. XPS analysis has also showed that pristine SWCNTs and ¹⁰⁰γ-OxA-SWCNTs contain both C–O and C=O bonds, while C–O bonds were not detected in the ¹⁰⁰γ-RedA-SWCNTs sample.

In addition to the XPS and FTIR analysis, we ran the TGA of the two most irradiated samples, ¹⁰⁰γ-OxA-SWCNTs and ¹⁰⁰γ-RedA-SWCNTs, in comparison with the pristine material (Figure S3, Supporting Information). The first outcome that has arisen from the TGA under N₂ is that the weight loss of the ¹⁰⁰γ-OxA-SWCNTs is higher than that of the ¹⁰⁰γ-RedA-SWCNTs (Figure S3.a, Supporting Information). This is translated in the greater amount of moieties that are attached on the sidewall of the CNTs. In Figure S3.b (Supporting Information), TGA spectra recorded under air show a difference in the thermal stability of the samples after the irradiation. That can be explained by the cutting of the CNTs for the case of ¹⁰⁰γ-OxA-SWCNTs and in general from a cleaning effect. In general, from XPS, FTIR, and TGA, we can conclude that the changes on the scaffold of the CNTs are bigger for the ¹⁰⁰γ-OxA-SWCNTs than in the case of ¹⁰⁰γ-RedA-SWCNTs.

According to structural investigation, gamma irradiation in oxidative media caused an increase in oxygen-containing functional groups. Because of the formation of oxidizing species (hydroxyl radicals, hydroperoxyl radicals, and hydrogen peroxide), C–C bonds in nanotube structure have ruptured, which results in the formation of additional functional groups in SWCNTs. Irradiation in reductive media caused elimination of C–O bonds in both carboxyl and hydroxyl functional groups in SWCNTs. These conditions affect only C–O bonds, while carbonyl functional groups stay intact.

3.3. Transmission Electron Microscopy. TEM images of pristine and irradiated nanotubes at a dose of 100 kGy in water mixed with IPA are presented in Figures S4.a,d (Supporting Information), relative to pristine nanotubes; it shows SWCNT bundles. The lengths of pristine nanotubes were between 500 and 2580 nm. The structure of SWCNT irradiated in reductive media (Figures S4.b,e, Supporting Information) is quite similar to the structure of pristine SWCNT and to the one from the sample in water with IPA.

The structure of SWCNTs irradiated in oxidative media is quite different (Figures S4.c,f, Supporting Information). Their length is in the range between 120 and 1210 nm.

TEM micrographs with higher magnification of same samples are shown in Figure 5. Intact structure is noticed for $_{100}\gamma$ -RedW-SWCNTs (Figure 5b). Yet for $_{100}\gamma$ -OxW-SWCNT sample, amorphous carbon can be detected as well as significantly shortened nanotubes (Figure 5c).

TEM analysis has shown the shortening of carbon nanotubes after irradiation with the high dose in oxidative media. Also, amorphous carbon is detected, which is in agreement with the very high I_D/I_G ratio calculated from Raman spectrum. On the other side, irradiation of SWCNTs in reductive media did not cause a shortening of nanotubes. The presence of IPA preserves SWCNT scaffold and protects them from cutting. These results are in a correspondence with Raman and XPS analysis.

3.4. Atomic Force Microscopy. The height profiles of pristine and gamma irradiated SWCNTs were measured by AFM. Representative results of these measurements are given in Figure 6. In Figure S5. (a, b, c) are high magnification AFM images with corresponding height profiles of pristine and gamma irradiated SWCNTs.

Figure 6a shows pristine nanotubes presented in compacted bundles with only one clear sharp peak in height profiles (Figure 6b). The height histogram (Figure 6c) indicates that an average height of nanotube bundles was 13 nm. In Figure 6d, the AFM image of $_{50}\gamma$ -OxA-SWCNTs sample is presented. Height profile analysis has shown that the bundle heights varied from 1 to 3 nm, which indicates separation of bundles into smaller ones or even into isolated SWCNTs (Figure 6e). The height histogram (Figure 6f) shows the most abundant fraction was nanotube bundles with the height of 2 nm. This result is in agreement with Raman analysis, which has shown debundling of carbon nanotubes at this medium and dose. AFM image and representative height profiles for the $_{50}\gamma$ -RedA-SWCNTs sample are presented in Figure 6g and h. The bundle heights are between 10 and 15 nm. In Figure 6i, the histogram shows that an average height of nanotube bundles was 12 nm. The height profile analysis revealed that bundle structure is preserved in reductive media during gamma irradiation.

4. CONCLUSIONS

A systematic analysis of pristine and gamma irradiated SWCNTs structure and morphology was presented. The analysis of all of the characterization techniques presents very interesting results for the gamma irradiation treatment on SWCNTs. The use of irradiation on the SWCNTs in reductive media leads to increasing fraction of sp^2 C atoms in the structure of SWCNTs. Also, selective reduction of C–O bonds in both carboxyl and hydroxyl groups in reductive media is observed. Irradiation of the SWCNTs in reductive media preserves both metallic and semiconducting SWCNTs. On the other hand, the same procedure in oxidative media yields to silencing of certain metallic nanotubes for the lower irradiation dose and the silencing of all of the small diameter SWCNTs for the highest dose.

■ ASSOCIATED CONTENT

Supporting Information

Tables S1–S5 and Figures S1–S5 as discussed in the text. This material is available free of charge via the Internet at <http://pubs.acs.org>.

■ AUTHOR INFORMATION

Corresponding Author

*Tel.: +381 11 3408 582. Fax: +381 11 344 0 100. E-mail: svetlanajovanovic@vinca.rs.

Notes

The authors declare no competing financial interest.

■ ACKNOWLEDGMENTS

This research was supported by the Ministry of Education, Science and Technological Development of the Republic of Serbia (project no. 172003). We acknowledge Prof. Maurizio Prato for valuable comments and discussion.

■ REFERENCES

- (1) Hirata, E.; Uo, M.; Takita, H.; Akasaka, T.; Watari, F.; Yokoyama, A. Multiwalled Carbon Nanotube-coating of 3D Collagen Scaffolds for Bone Tissue Engineering. *Carbon* **2011**, *49*, 3284–3291.
- (2) Dresselhaus, M. S.; Dresselhaus, G.; Charlier, J. C.; Hernandez, E. Electronic, Thermal and Mechanical Properties of Carbon Nanotubes. *Philos. Trans. R. Soc. London, Ser. A* **2004**, *362*, 2065–2098.
- (3) Tasis, D.; Tagmatarchis, N.; Bianco, A.; Prato, M. Chemistry of Carbon Nanotubes. *Chem. Rev.* **2006**, *106*, 1105–1136.
- (4) Li, X. M.; Fan, Y. B.; Watari, F. Current Investigations into Carbon Nanotubes for Biomedical Application. *Biomed. Mater.* **2010**, *5*, 022001.
- (5) Park, G. E.; Webster, T. J. A Review of Nanotechnology for the Development of Better Orthopedic Implants. *J. Biomed. Nanotechnol.* **2005**, *1*, 18–29.
- (6) Mattson, M. P.; Haddon, R. C.; Rao, A. M. Molecular Functionalization of Carbon Nanotubes and Use as Substrates for Neuronal Growth. *J. Mol. Neurosci.* **2000**, *14*, 175–182.
- (7) Dresselhaus, M. S.; Dresselhaus, G.; Jorio, A. Unusual Properties and Structure of Carbon Nanotubes. *Annu. Rev. Mater. Res.* **2004**, *34*, 247–278.
- (8) Liu, Z.; Robinson, J. T.; Tabakman, S. M.; Yang, K.; Dai, H. J. Carbon Materials for Drug Delivery & Cancer Therapy. *Mater. Today* **2011**, *14*, 316–323.
- (9) Bauer, L. A.; Birenbaum, N. S.; Meyer, G. J. Biological Applications of High Aspect Ratio Nanoparticles. *J. Mater. Chem.* **2004**, *14*, 517–526.
- (10) Azamian, B. R.; Davis, J. J.; Coleman, K. S.; Bagshaw, C. B.; Green, M. L. H. Bioelectrochemical Single-Walled Carbon Nanotubes. *J. Am. Chem. Soc.* **2002**, *124*, 12664–12665.
- (11) Upadhyayula, V. K. K.; Deng, S. G.; Mitchell, M. C.; Smith, G. B. Application of Carbon Nanotube Technology for Removal of Contaminants in Drinking Water: A Review. *Sci. Total Environ.* **2009**, *408*, 1–13.
- (12) Markovic, Z. M.; Harhaji-Trajkovic, L. M.; Todorovic-Markovic, B. M.; Kepic, D. P.; Arsikin, K. M.; Jovanovic, S. P.; Pantovic, A. C.; Dramicanin, M. D.; Trajkovic, V. S. In Vitro Comparison of The Photothermal Anticancer Activity of Graphene Nanoparticles and Carbon Nanotubes. *Biomaterials* **2011**, *32*, 1121–1129.
- (13) Son, S. J.; Bai, X.; Lee, S. Inorganic Hollow Nanoparticles and Nanotubes in Nanomedicine. Part 2: Imaging, Diagnostic, And Therapeutic Applications. *Drug Discovery Today* **2007**, *12*, 657–663.
- (14) Zhou, F. F.; Xing, D.; Ou, Z. M.; Wu, B. Y.; Resasco, D. E.; Chen, W. R. Cancer Photothermal Therapy in the Near-Infrared Region by Using Single-Walled Carbon Nanotubes. *J. Biomed. Opt.* **2009**, *14*, 021009.
- (15) Vazquez, E.; Giacalone, F.; Prato, M. Non-Conventional Methods and Media for the Activation and Manipulation of Carbon Nanoforms. *Chem. Soc. Rev.* **2013**, *43*, 58–69.
- (16) Xu, Z. W.; Chen, L.; Zhou, B. M.; Li, Y. L.; Li, B. D.; Niu, J. R.; Shan, M. J.; Guo, Q. W.; Wang, Z.; Qian, X. M. Nano-Structure and Property Transformations of Carbon Systems under Gamma-Ray Irradiation: A Review. *Rsc Advances* **2013**, *3*, 10579–10597.

- (17) Peng, J.; Qu, X. X.; Wei, G. S.; Li, J. Q.; Qiao, J. L. The Cutting of MWNTs using Gamma Radiation in the Presence of Dilute Sulfuric Acid. *Carbon* **2004**, *42*, 2741–2744.
- (18) Jung, C. H.; Kim, D. K.; Choi, J. H.; Nho, Y. C.; Shin, K.; Suh, D. H. Shortening of Multi-Walled Carbon Nanotubes by Gamma-Irradiation in the Presence of Hydrogen Peroxide. *Nucl. Instr. Meth. Phys.* **2008**, *266*, 3491–3494.
- (19) Chen, S. M.; Wu, G. Z.; Liu, Y. D.; Long, D. W. Preparation of Poly(Acrylic Acid) Grafted Multiwalled Carbon Nanotubes by a Two-Step Irradiation Technique. *Macromolecules* **2006**, *39*, 330–334.
- (20) Guo, J. X.; Li, Y. G.; Wu, S. W.; Li, W. X. The Effects of Gamma-Irradiation Dose on Chemical Modification of Multi-Walled Carbon Nanotubes. *Nanotechnology* **2005**, *16*, 2385–2388.
- (21) Jovanovic, S. P.; Markovic, Z. M.; Kleut, D. N.; Romcevic, N. Z.; Trajkovic, V. S.; Dramicanin, M. D.; Markovic-Todorovic, B. M. A Novel Method for the Functionalization of Gamma-Irradiated Single Wall Carbon Nanotubes with DNA. *Nanotechnology* **2009**, *20*, 445602.
- (22) Hulman, M.; Skakalova, V.; Roth, S.; Kuzmany, H. Raman Spectroscopy of Single-Wall Carbon Nanotubes and Graphite Irradiated by Gamma Rays. *J. Appl. Phys.* **2005**, *98*, 024311.
- (23) Kleut, D.; Jovanovic, S.; Markovic, Z.; Kepic, D.; Tosic, D.; Romcevic, N.; Marinovic-Cincovic, M.; Dramicanin, M.; Holclajtner-Antunovic, I.; Pavlovic, V.; Drazic, G.; Milosavljevic, M.; Markovic-Todorovic, B. Comparison of Structural Properties of Pristine and Gamma Irradiated Single-Wall Carbon Nanotubes: Effects of Medium and Irradiation Dose. *Mater. Charact.* **2012**, *72*, 37–45.
- (24) Xu, Z. W.; Chen, L.; Liu, L. S.; Wu, X. Q.; Chen, L. Structural Changes in Multi-Walled Carbon Nanotubes Caused by Gamma-Ray Irradiation. *Carbon* **2011**, *49*, 339–351.
- (25) Xu, Z. W.; Min, C. Y.; Chen, L.; Liu, L. S.; Chen, G. W.; Wu, N. Modification of Surface Functionality and Interlayer Spacing of Multi-Walled Carbon Nanotubes Using Gamma-Rays. *J. Appl. Phys.* **2011**, *109*, 054303.
- (26) Li, B.; Feng, Y.; Ding, K. W.; Qian, G.; Zhang, X. B.; Zhang, J. C. The Effect of Gamma Ray Irradiation on the Structure of Graphite and Multi-Walled Carbon Nanotubes. *Carbon* **2013**, *60*, 186–192.
- (27) Temgire, M. K.; Joshi, S. S. Optical and Structural Studies of Silver Nanoparticles. *Radiat. Phys. Chem.* **2004**, *71*, 1039–1044.
- (28) Sheikh, N.; Akhavan, A.; Kassaee, M. Z. Synthesis of Antibacterial Silver Nanoparticles by Gamma-Irradiation. *Physica E* **2009**, *42*, 132–135.
- (29) Belloni, J.; Mostafavi, M.; Remita, H.; Marignier, J. L.; Delcourt, M. O. Radiation-Induced Synthesis of Mono- and Multi-Metallic Clusters and Nanocolloids. *New J. Chem.* **1998**, *22*, 1239–1255.
- (30) Marković, Z.; Kepić, D.; Antunović, I. H.; Nikolić, M.; Dramičanin, M.; Cincović, M. M.; Marković, B. T. Raman Study of Single Wall Carbon Nanotube Thin Films Treated by Laser Irradiation, Dynamic and Isothermal Oxidation. *J. Raman Spectrosc.* **2012**, *43*, 1413–1422.
- (31) Dresselhaus, M. S.; Jorio, A.; Hofmann, M.; Dresselhaus, G.; Saito, R. Perspectives on Carbon Nanotubes and Graphene Raman Spectroscopy. *Nano Lett.* **2010**, *10*, 751–758.
- (32) Dresselhaus, M. S.; Jorio, A.; Souza, A. G.; Saito, R. Defect Characterization in Graphene and Carbon Nanotubes Using Raman Spectroscopy. *Philos. Trans. R. Soc. London, Ser. A* **2010**, *368*, 5355–5377.
- (33) Souza, A. G.; Jorio, A.; Samsonidze, G. G.; Dresselhaus, G.; Pimenta, M. A.; Dresselhaus, M. S.; Swan, A. K.; Unlu, M. S.; Goldberg, B. B.; Saito, R. Competing Spring Constant Versus Double Resonance Effects on the Properties of Dispersive Modes in Isolated Single-Wall Carbon Nanotubes. *Phys. Rev. B* **2003**, *67*, 035427–1–035427–7.
- (34) Brown, S. D. M.; Jorio, A.; Corio, P.; Dresselhaus, M. S.; Dresselhaus, G.; Saito, R.; Kneipp, K. Origin of the Breit-Wigner-Fano Lineshape of the Tangential G-Band Feature of Metallic Carbon Nanotubes. *Phys. Rev. B* **2001**, *63*, 155414–1–155414–8.
- (35) Shin, H. J.; Kim, S. M.; Yoon, S. M.; Benayad, A.; Kim, K. K.; Kim, S. J.; Park, H. K.; Choi, J. Y.; Lee, Y. H. Tailoring Electronic Structures of Carbon Nanotubes by Solvent with Electron-Donating and -Withdrawing Groups. *J. Am. Chem. Soc.* **2008**, *130*, 2062–2066.
- (36) Yu, B.; Hou, P. X.; Li, F.; Liu, B. L.; Liu, C.; Cheng, H. M. Selective Removal of Metallic Single-Walled Carbon Nanotubes by Combined in Situ and Post-Synthesis Oxidation. *Carbon* **2010**, *48*, 2941–2947.
- (37) LaVerne, J. A. OH Radicals and Oxidizing Products in the Gamma Radiolysis of Water. *Radiat. Res.* **2000**, *153*, 196–200.
- (38) Draganic, I. G. Radiolysis of Water: A Look at Its Origin and Occurrence in the Nature. *Radiat. Phys. Chem.* **2005**, *72*, 181–186.
- (39) Dresselhaus, M. S.; Dresselhaus, G.; Jorio, A.; Souza Filho, A. G.; Saito, R. Raman Spectroscopy on Isolated Single Wall Carbon Nanotubes. *Carbon* **2002**, *40*, 2043–2061.
- (40) Kataura, H.; Kumazawa, Y.; Maniwa, Y.; Umezawa, I.; Suzuki, S.; Ohtsuka, Y.; Achiba, Y. Optical Properties of Single-Wall Carbon Nanotubes. *Synth. Met.* **1999**, *103*, 2555–2558.
- (41) Quintana, M.; Ke, X. X.; Van Tendeloo, G.; Meneghetti, M.; Bittencourt, C.; Prato, M. Light-Induced Selective Deposition of Au Nanoparticles on Single-Wall Carbon Nanotubes. *ACS Nano* **2010**, *4*, 6105–6113.
- (42) Wepasnick, K. A.; Smith, B. A.; Bitter, J. L.; Fairbrother, D. H. Chemical and Structural Characterization of Carbon Nanotube Surfaces. *Anal. Bioanal. Chem.* **2010**, *396*, 1003–1014.
- (43) Syrgiannis, Z.; La Parola, V.; Hadad, C.; Lucio, M.; Vazquez, E.; Giacalone, F.; Prato, M. An Atom-Economical Approach to Functionalized Single-Walled Carbon Nanotubes: Reaction with Disulfides. *Angew. Chem., Int. Ed.* **2013**, *52*, 6480–6483.
- (44) Criado, A.; Gomez-Escalona, M. J.; Fierro, J. L. G.; Urbina, A.; Pena, D.; Guitian, E.; Langa, F. Cycloaddition of Benzyne to SWCNT: towards CNT-Based Paddle Wheels. *Chem. Commun.* **2010**, *46*, 7028–7030.
- (45) Jung, A.; Graupner, R.; Ley, L.; Hirsch, A. Quantitative Determination of Oxidative Defects on Single Walled Carbon Nanotubes. *Phys. Status Solidi B* **2006**, *243*, 3217–3220.
- (46) Rodríguez, J. L.; Valenzuela, M. A.; Poznyak, T.; Lartundo, L.; Chairez, I. Reactivity of NiO for 2,4-D Degradation with Ozone: XPS Studies. *J. Hazard. Mater.* **2013**, *262*, 472–481.
- (47) Baggetto, L.; Dudney, N. J.; Veith, G. M. Surface Chemistry of Metal Oxide Coated Lithium Manganese Nickel Oxide Thin Film Cathodes Studied by XPS. *Electrochim. Acta* **2013**, *90*, 135–147.